# Diffusion through Fibre Networks

E.K.O. HELLÉN, J.A. KETOJA, K.J. NISKANEN and M.J. ALAVA

*We study gas diffusion through computer-generated random fibre networks using random walk simulations. The simulation results are consistent with steady-state experiments. The comparison of the simulated time-dependent diffusion flux with one-dimensional diffusion theory suggests that the latter is invalid at low porosities and low thicknesses. We also find that, if sorption is relevant, steady-state measurements of the diffusion constant combined with the one-dimensional diffusion theory are not enough to predict the dynamic evolution of diffusion flux. Our results demonstrate that gas diffusion through uncoated paper and board sheets can be simulated using model fibre networks, including the effects of fibre sorption.*

*Nous avons étudié la diffusion du gaz dans des réseaux de fibres aléatoires sur ordinateur à l'aide de simulations de marche aléatoire. Les résultats des simulations sont conformes aux essais à l'état stationnaire. La comparaison du flux de diffusion diachronique simulé avec la théorie de la diffusion unidimensionnelle suggère que cette dernière est invalide à faible porosité et à faible épaisseur. Nous avons aussi trouvé que, si la sorption est pertinente, les mesures à l'état stationnaire de la constante de diffusion combinées à la théorie de la diffusion unidimensionnelle ne suffisent pas pour prédire l'évolution dynamique du flux de diffusion. Nos résultats démontrent que la transporisation à travers des feuilles de carton ou de papier non couché peut être simulée à l'aide de réseaux de fibres modélisés, y compris les effets de la sorption des fibres.*

## INTRODUCTION

Understanding diffusive transport is important in many papermaking operations and end uses of paper and board. Examples range from the moisture and heat diffusion in drying, coating, calendering and printing to the migration of organic compounds in food packaging materials. These processes are often described using the classical one-dimensional diffusion theory [1]. The material properties of paper enter only through the diffusion constant. Since reliable measurements of the diffusion constant are very tedious, theoretical models and numerical simulation methods would be useful in the evaluation of different furnish compositions and sheet structures.

Often the applicability of the one-dimensional diffusion theory to paper and board is not obvious. For example, sorption can alter the short-time transient evolution of the diffusion flux without any effects observed in the long-time steady-state flux that is usually measured. Thus the diffusion constant (measured, by definition, in steady-state conditions) is insufficient if one wants to understand dynamic diffusion processes with sorption. This includes all applications where water is applied or removed from a running paper web. To our knowledge, no work has been published that describes how the dynamic evolution of diffusion flux depends on fibre properties and sheet structure.

The inhomogeneous structure of paper and board complicates the analysis of diffusion. The average diffusion constant of a relatively thick sheet can be quite different from the diffusion constant of a thin sheet or a thin layer of a thick sheet. Just consider the role of formation. This calls again for effective tools to analyze and predict diffusion in real situations.

In this work, we study diffusive transport through paper sheets using random walk simulations and one-dimensional diffusion theory. Our analysis includes sorption. We construct the fibre networks for the diffusion simulations using a model that is known to produce structures that closely resemble real paper [2,3]. This means that we can directly determine the effect of paper structure on diffusion. To simulate the diffusion process we let random walkers move through the sheet. Sorption corresponds to a time delay for walkers that hit a fibre surface. Our simulations mimic a situation where all the molecules are initially on, say, the lower side of the sheet and then diffuse to the top side. The simulated flux of molecules to the top side can be directly compared with experiments. The one-dimensional diffusion theory considers the average movement of molecules in the thickness direction of the sheet. When fibre sorption is included, we obtain two coupled linear differential equations. We solve them with the Laplace transformation.

We also summarize the construction of the random fibre networks. The random walk simulations and the one-dimensional theory are described. We compare both approaches to each other and also to the earlier experimental data of water vapour diffusion.

JPPS

E.K.O. Hellén and M.J. Alava
Laboratory of Physics
Helsinki Univ. Technol.
PO Box 110
FIN-02150 HUT, Finland
J.A. Ketoja and K.J. Niskanen
KCL Sci. and Consulting
PO Box 70
FIN-02151 Espoo, Finland
(jukka_ketoja@kcl.fi)

## FIBRE NETWORKS

### Network Generation

The simulation networks are constructed using the KCL-PAKKA program that produces planar structures of flexible fibres [2,3]. In the model, fibres of rectangular cross-section are deposited randomly (including random orientation) on a flat substrate surface. The xy surface is discretized in square cells $i$ of area $\Delta^2$. Fibre length $l_f$ and width $w_f$ are multiples of $\Delta$. The edges of each fibre are deformed so that the fibre covers completely $l_f w_f / \Delta^2$ cells. This is done by moving fibre material between partially covered cells while keeping the mean orientation of the fibre constant.

Each fibre is let to settle freely as low as possible without deforming the underlying sheet. The vertical coordinates $z_i$ describing the location of the top surface of a fibre above the

cell $i$ are calculated from the equation

$$\frac{G_f t_f \Delta}{N_i} \sum_{j=1}^{N_i} \frac{z_j - z_i}{\Delta} = p\Delta^2 \quad (1)$$

where the sum is over the $N_i$ nearest neighbour cells around the cell $i$ that are covered by the same fibre. $t_f$ and $G_f$ are, respectively, the thickness and shear modulus of the fibre. The fibre bends under the uniform pressure $p$ that represents all the compressive effects of wet pressing to reach an equilibrium given by Eq. (1). An additional constraint is applied to prevent the fibre from penetrating through the underlying sheet structure.

The present version of the KCL-PAKKA differs from the earlier in two respects: (1) fibre orientations are isotropically distributed in xy directions, and (2) fibre bending is calculated from the force balance instead of constraining the maximum deflection $z_i - z_j$ as before [2,3]. We have checked that the network structure is insensitive to these changes.

We restrict ourselves to sheets that consist of only one type of fibre. The sheet is built on a flat substrate of 300 × 300 cells of size $\Delta$ = 10 μm. The corresponding real paper sheet has the area 0.09 cm$^2$. Periodic boundary conditions are applied to fibres that cross the boundaries of the flat substrate. The fibre properties are: density (including lumen in the fibre volume) 1400 kg/m$^3$, length 2 mm, thickness 4.3 μm, width 40 μm, and the ratio of pressure over fibre shear modulus $p/G_f = 0.075 - 0.38$. Notice that this parameter is used to control the porosity while the others are kept fixed; the values used lead to sheet densities 400–1000 kg/m$^3$ and porosities 0.3–0.7.

### Sheet Thickness and Porosity

In order to relate the simulations with the one-dimensional model and experiments, we have to define the thickness and porosity of the KCL-PAKKA sheets used in the simulations. The definition is complicated by the surface roughness and possible holes in thin sheets. For example, the thickness of the sheet could be defined as the maximum distance $z_{max}$ between the bottom and top surface of the sheet. Another choice would be the average value of local thicknesses. This is often called the effective thickness. It is seldom measured in practice. For comparison with experiments we define the apparent thickness $a$ of the simulated sheets so that 80% of local thickness values are below $a$. According to our experience, this definition mimics best the real thickness measurement with a hard platen.

There are also several candidates for porosity: (1) the pore volume fraction $\phi_{max}$ between $z = 0$ and $z = z_{max}$; (2) the pore volume fraction $\phi_{ave}$ between the local bottom and top surfaces of the sheet; and (3) the apparent porosity $\phi_{app} = 1 - \rho_{app}/\rho_f$, where $\rho_f$ is fibre density and $\rho_{app}$ equals grammage divided by $a$. Due to high roughness of the top surfaces of KCL-PAKKA sheets, the first choice clearly overestimates the physical porosity that controls diffusion. The second definition in turn ignores holes through the sheet so that $\phi_{ave}$ goes to zero when grammage decreases. This underestimates the physical porosity in the sense that diffusion through the holes increases when grammage decreases. If we used this definition for porosity, all simulated diffusion constants would be sensitive to grammage even at the levels of 60–120 g/m$^2$. The third definition $\phi_{app}$ is in line with our definition of the apparent thickness $a$. Moreover, the analogous quantity is easily measurable in experiments. We will use this definition and denote it by simple $\phi$ from this point on when it causes no confusion.

In the diffusion simulation, molecules travel from $z = 0$ to $z_{max}$ giving the highest point of the sheet. This distance is larger than $a$ and therefore the simulations give, in principle, an underestimate of the diffusion constant which assumes that sheet thickness is $a$. However, the error is very small because extra distance in the simulations (proportional to $\sqrt{a}$) consists mainly of diffusion in free space. Thus for all realistic porosities and sheet thicknesses, the diffusion time from $a$ to $z_{max}$ is much smaller than the time from 0 to $a$. For example, when $a$ = 90 μm the extra time is ≤ 4% when $\phi \le 0.7$.

## RANDOM WALK SIMULATION

Diffusion at low gas concentrations can be studied by random walks [4], especially in complex pore structures. In the simulation we track the flux $H(t)$ of molecules as they emerge from the exit side (top surface) of the sheet. At long times, $H(t)$ coincides with the flux given by the one-dimensional diffusion equation. We use this equivalence to determine the diffusion constant $D$ from the random walk simulations. Sorption does not affect the asymptotic, steady-state flux at large times. Therefore sorption does not affect the diffusion constant.

For the efficiency of the diffusion simulations we divide the fibre network into a simple cubic lattice with the lattice constant $\delta$. This discretization has to be finer than in the flat substrate ($\Delta$ = 10 μm) since the geometry in the vertical direction has to be given more accurately. On the other hand $\delta$ should not be too small to avoid heavy computations. We have used $\delta$ = 2 μm since simulations with $\delta$ = 1 μm gave the same results. When forming the cubic lattice, each lattice site is occupied by a fibre with a probability equal to the volume fraction of the site that is inside the fibre. For the grammage 80 g/m$^2$, there are 8 × 10$^8$ sites in a typical cubic lattice, requiring approximately 50 Mb of RAM memory.

The molecules perform random walks in the free sites between the fibres. At each time step each molecule sees a local configuration $C$ of free nearest neighbour sites in the lattice (≤6 in the simple cubic lattice). When modeling sorption and desorption, we assume for simplicity that desorption takes place at the same fibre surface site as sorption. Notice that, since the fibres in the network are aligned mainly horizontally, desorption would always occur roughly at the same height even if the molecule diffused along the fibre wall or inside the fibre lumen. Then the sorption/desorption processes can be described as a time delay in the random walk through empty sites.

It is easy to calculate the average jump time $\bar{t}(C)$ that it takes for a molecule to move from a given configuration $C$ to a free nearest neighbour site. Let $\hat{\lambda}$ and $\hat{\mu}$ denote the sorption and desorption constants, the probability of sorption and desorption in unit time. After a time $t$ a molecule can be in three possible states: (I) It may still be on the empty site we are considering, (II) it may be sorbed, or (III) it may be on some of the nearest neighbour empty sites. In the Markov process language, state III is an absorbing one and the average leaving time that we are interested in is the average number of jumps required to reach this state. Here we normalize the time so that in free space a molecule takes one step in a unit time.

To construct the transition probability matrix, $P_T$, we have to consider the probabilities to go from one state to another. If, for example, a molecule is in state I and $b$ (6–$b$) of the nearest neighbour sites are filled with fibres (empty), the probabilities to go to states I, II, and III are $b(1-\hat{\lambda})/6$, $(b\hat{\lambda}/6)$, and $(1 - b/6)$, respectively. By similar considerations we end up with the following transition probability matrix between states:

$$P_T = \begin{pmatrix} b1 - \hat{\lambda}/6 & b\hat{\lambda}/6 & 1 - b/6 \\ \hat{\mu} & (1-\hat{\mu}) & 0 \\ 0 & 0 & 1 \end{pmatrix} \quad (2)$$

Next, we neglect the row and the column including the absorbing state and construct the matrices

$$Q = \begin{pmatrix} b1 - \hat{\lambda}/6 & b\hat{\lambda}/6 \\ \hat{\mu} & (1-\hat{\mu}) \end{pmatrix} \quad (3)$$

and $N = (I - Q)^{-1}$, where $I$ is the identity matrix. Let $N_{ij}$ denote the matrix elements of $N$. Then the average leaving time from the state I is [4]

$$\bar{t}(C) = N_{11} + N_{12} = \frac{6 + \hat{v}b(C)}{6 - b(C)} \quad (4)$$

where the dependence of $b$ on the configuration is explicitly shown and $\hat{v} = \hat{\lambda}/\hat{\mu}$. It is straightforward to extend the above calculation to a situation where the sheet consists of many fibre types which may have different sorption properties. The only change in Eq. (4) is that the factor $\hat{v}b$ in the numerator will be changed to $\sum_i \hat{v}_i k_i(C)$, where $\hat{v}_i = \hat{\lambda}_i/\hat{\mu}_i$ is the sorption to desorption ratio for the fibre type $i$, $k_i$ is the number of fibres of type $i$ in the nearest neighbour sites, and the sum runs over all the fibre types.

All the molecules start the random walk just below the sheet at $z = 0$. Each walker is subject to periodic boundary conditions in the horizontal xy direction. The walk is terminated either when the molecule emerges through the surface $z = z_{max}$ for the first time or when a prior time limit, $t_{term}$, is exceeded. Here $z_{max}$ denotes the heighest point of the sheet. The termination time $t_{term}$ has to be used since the average penetration time for a single walker is infinite. We varied $t_{term}$ depending on the range of times $t < t_{term}$ in which the simulation results were to

be plotted. This range was chosen to be much larger than the time at which the penetration flux obtained its maximum value.

Another issue in the simulations is the number of the penetrating random walkers. When this number is increased, the calculated first-passage time distribution (see below) becomes smoother. We found that with 10 000 penetrating random walkers the simulated distribution was practically indistinguishable from the analytical solution (refer to the Analytical Solutions section) for $t < t_{term}$.

From the simulations we obtain the conditional first-passage time distribution $F(z(t) = L + 1|z(0) = 0)$ when all the molecules start their random walk just below the bottom of the sheet. Here $L = z_{max}/\delta$ is the maximum sheet thickness in the cubic lattice units. The distribution $F$ is related to the first-passage time distribution $f(t)$ in the practical case where the molecules have a uniform initial concentration $c$ in the entire half space below the sheet ($z \le 0$):

$$f(t) = c \sum_{n=0}^{\lceil t-L-1 \rceil} F\big(z(t-n) = L+1 \big| z(0) = 0\big) \times \sum_{z_0=0}^{n} P_{z_0}(n) \qquad (5)$$

Here $\lceil x \rceil$ denotes the integer part of $x$ and $P_{z_0}(n)$ is the probability that the first passage through the plane $z = 0$ occurs at the $n$th step assuming that the walk starts from $z = -z_0$. The flux $H(t)$ exiting the sheet is obtained directly from the first-passage time distribution: $H(t) = f(t/\tau)/\tau$, where $\tau = \delta^2/(6D_g)$ is the time the random walker spends in an empty site of size $\delta$.

The distribution $P_{z_0}(n)$ has the following analytical expression (see Appendix A):

$$P_{z_0}(n) = \left(\frac{2}{3}\right)^n z_0 4^{z_0} \sum_{n_z=z_0}^{\lceil (n+z_0)/2 \rceil} \frac{4^{-2n_z}(n-1)!}{n_z!\,(n_z-z_0)!\,(n-2n_z+z_0)!} \qquad (6)$$

For large $n > 1500$, we use the continuous approximation

$$P_{z_0}(n) \approx \frac{z_0}{\sqrt{2\pi/3}} n^{-3/2} e^{-3z_0^2/2n} \qquad (7)$$

We employ the distribution $P_{z_0}(n)$ also in the actual simulations because it would be a waste of time to allow the molecule to wander around in the free space below the sheet. Instead, if the molecule goes down to height $z = -1$, it will be returned to the level $z = 0$ just below the sheet after a time taken from the distribution $P_1(n)$. The return position in the xy plane is random according to a spatial distribution which can be calculated analytically as well (see Appendix B). Since the discrete form is quite complicated we give here only the continuous approximation

$$p_1(R;t) = 2\pi(2\pi/3)^{-3/2} t^{-5/2} R e^{-3(1+R^2)/2t} \qquad (8)$$

for return at a planar distance $R$ from the site where the molecule moved downwards for the first time at $t = 0$.

## ONE-DIMENSIONAL THEORY

### Basic Equations

The one-dimensional model includes the diffusion in the interfibre pore space and the sorption into and desorption from fibre walls. Diffusion along fibres in the thickness direction is excluded. The $z$-coordinate defines the position in the vertical thickness direction (see Fig. 1). The sheet fills the space in the interval $0 \le z \le a$. Here $a$ denotes the apparent sheet thickness defined in the section Sheet Thickness and Porosity. The free space below and above the sheet is assumed to be infinite. The volume and porosity of the sheet are $V$ and $\phi$, respectively. The concentrations of molecules in the pore space and fibre space, $C_p(z,t)$ and $C_f(z,t)$, are defined with respect to the total volume $V$. Thus if $M_p$ ($M_f$) denotes the amount of molecules in the pore (fibre) space of volume $V_p = \phi V$ ($V_f = (1 - \phi)V$), the concentrations read as $C_p(z) = M_p(z)/V$ and $C_f(z) = M_f(z)/V$ (here the unit of $M_p$ and $M_f$ and thus the unit of concentration can be chosen freely).

The concentration of molecules in the pore space at a certain height, $C_p(z)$, changes when a molecule diffuses from one height to another. It also changes when the molecule is sorbed or desorbed, in which case the rate of the change of the concentration in the pore space is equal to the change of the concentration in the fibre space, $\partial C_f / \partial t$, since the total amount of molecules is conserved. On the other hand, $C_f$ changes only through sorption and desorption as we assume that diffusion takes place only in the pore space. When a molecule is bound by a fibre at the height $z$, it will be later released at the same height. The sorption rate can be assumed to be proportional to the number of molecules near a fibre wall and thus to $C_p$. In the same way the rate of desorption is proportional to $C_f$. Thus the diffusion and sorption process is represented by the coupled differential equations

$$\frac{\partial C_p(z,t)}{\partial t} = D\frac{\partial^2 C_p(z,t)}{\partial z^2} - \frac{\partial C_f(z,t)}{\partial t} \qquad (9)$$

$$\frac{\partial C_f(z,t)}{\partial t} = \lambda C_p(z,t) - \mu C_f(z,t) \qquad (10)$$

where $D$ is the diffusion constant and $\lambda$ and $\mu$ describe the sorption and desorption rates. In free space under the sheet the concentration $C(z,t)$ satisfies the standard diffusion equation

$$\frac{\partial C(z,t)}{\partial t} = D_g \frac{\partial^2 C(z,t)}{\partial z^2} \qquad (11)$$

where $D_g$ is the molecular diffusion constant in the free space (e.g. air).

Initially all the molecules are below the sheet in a constant concentration

$$C(z,0) = C_0 \quad (z < 0) \qquad (12)$$

$$C_p(z,0) = C_f(z,0) = 0 \quad (0 < z \le a) \qquad (13)$$

which remains unaltered for finite times far away from the sheet:

$$\lim_{z\to-\infty} C(z,t) = C_0 \quad (t > 0) \qquad (14)$$

At the bottom sheet surface, the flux of molecules obviously has to be continuous

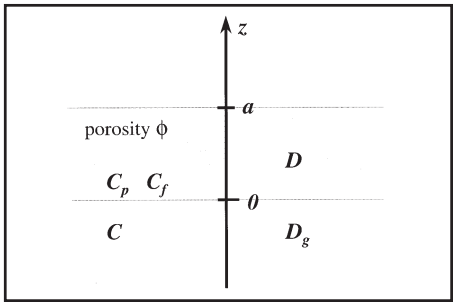


**Fig. 1. The geometry of the continuous diffusion model.**

$$D\frac{\partial C_p}{\partial z} = D_g \frac{\partial C}{\partial z} \quad (z = 0, t > 0) \qquad (15)$$

whereas the concentration itself is discontinuous

$$C_p(0,t) = \phi C(0,t) \quad (t > 0) \qquad (16)$$

The discontinuity is a consequence of the pore concentration being defined with respect to the total volume rather than to the pore volume. The top sheet surface is taken to be fully absorbing

$$C_p(a,t) = 0 \quad (t > 0) \qquad (17)$$

such as in the simulations, so that no molecules return to the sheet once they have penetrated it for the first time.

### Analytical Solutions

In the absence of sorption ($\lambda = \mu = 0$), it is straightforward to apply the Laplace transformation to solve Eqs. (9) and (11) for the concentrations $C_p$ and $C$ under the conditions of the previous section [6]. Here we only give the final solution for $C_p(z,t)$ when $t > 0$:

$$C_p(z,t) = \frac{\phi C_0}{1+\phi\sqrt{D/D_g}} \sum_{n=0}^{\infty}(-1)^n \alpha^n \times \left[\operatorname{erfc}\left(\frac{2na+z}{2\sqrt{Dt}}\right) - \operatorname{erfc}\left(\frac{2(n+1)a-z}{2\sqrt{Dt}}\right)\right] \qquad (18)$$

$$\alpha = \frac{\phi - \sqrt{D_g/D}}{\phi + \sqrt{D_g/D}} \qquad (19)$$

and $\operatorname{erfc}(x)$ is the complementary error function. From Eq. (18) it is easy obtain the flux at the top sheet boundary:

$$-D\left.\frac{\partial C_p}{\partial z}\right|_{z=a} = \frac{2\phi C_0\sqrt{D}}{(1+\phi\sqrt{D/D_g})\sqrt{\pi t}} \times \sum_{n=0}^{\infty}(-1)^n \alpha^n \exp\left(-\frac{(2n+1)^2 a^2}{4Dt}\right) \qquad (20)$$

Equation (20) shows that the flux is practically zero until a time proportional to $a^2/D$ after which it grows rapidly. After the maximum flux, there is a very slow decrease coming from the factor $1/\sqrt{t}$. In experiments, one usually measures the total amount of molecules which

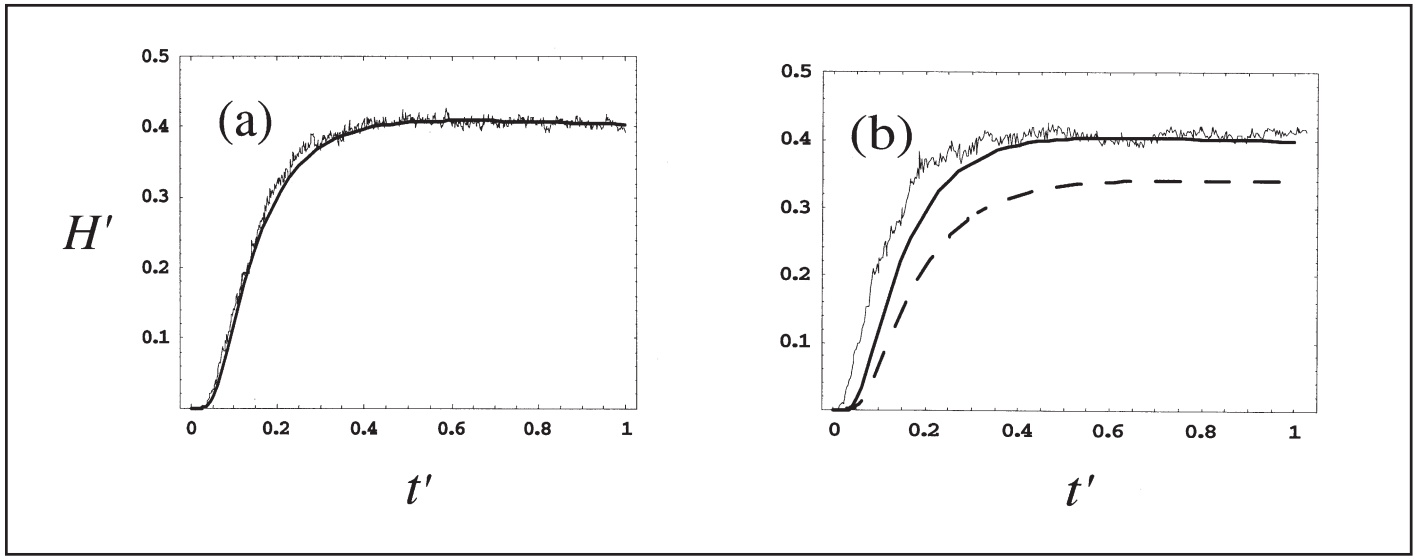


**Fig. 2. The comparison of the simulated flux (rough line) and the one obtained from Eq. (20) (smooth line) in the absence of sorption. Here $t' = Dt/a^2$ and $H' = Ha/(C_0D)$ are the dimensionless time and flux. In (a) the parameter values are $\phi_{app} = 0.458$, $a = 369$ μm, $D = 0.0545\ D_g$. In (b) $\phi_{app} = 0.463$, $a = 47$ μm, and the diffusion constant obtained by fitting the flux tail (smooth solid curve) is $D = 0.0659\ D_g$. The dashed curve shows the flux of the one-dimensional theory obtained using the same diffusion constant as in (a).**

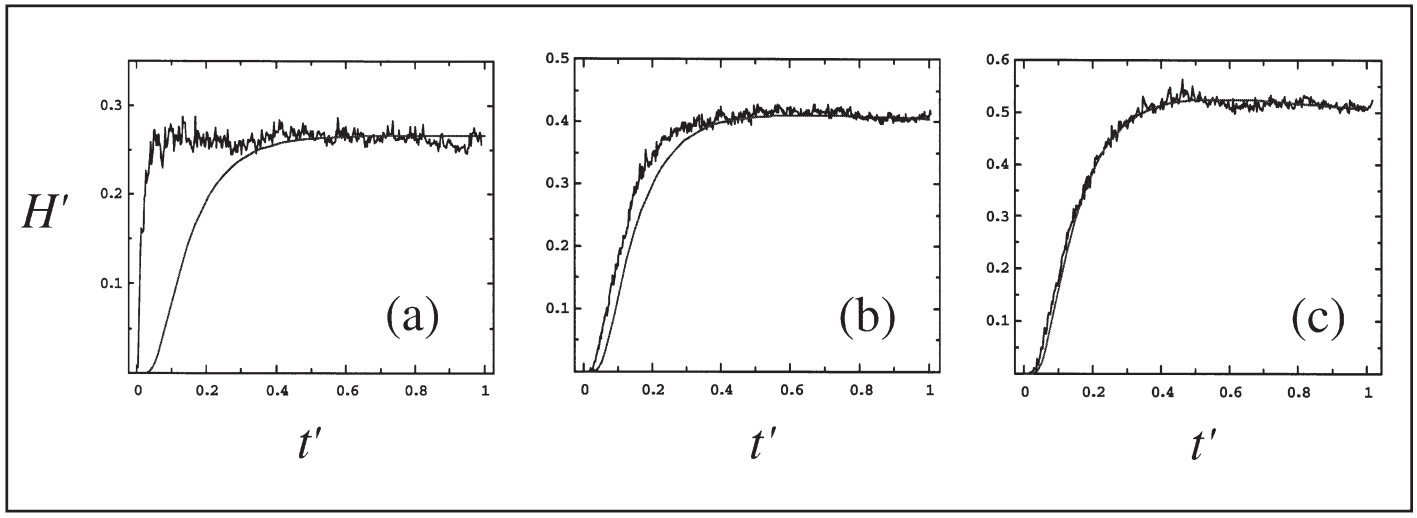


**Fig. 3. Simulated flux (rough line) compared with the one obtained from the one-dimensional diffusion theory (smooth line) for the porosities $\phi_{app} = 0.270$ (a), $\phi_{app} = 0.459$ (b), and $\phi_{app} = 0.685$ (c). In all cases, the apparent thickness is $a = 140 \pm 3$ μm. The diffusion constant $D$ in each case is obtained by matching the one-dimensional theory to the saturation flux of the simulation.**

have penetrated the sheet at a certain time. This can be obtained by simply integrating the flux in Eq. (20).

For sorption without desorption ($\mu = 0, \lambda \neq 0$) the transformation $C_p(z,t) = e^{-\lambda t}u(z,t)$ can be used to cast Eq. (9) into the standard diffusion equation form for $u$ with slightly modified boundary conditions at $z = 0$. When both $\lambda$ and $\mu$ are finite, the system of equations becomes more complex. However, the differential equations remain linear, enabling one to apply the Laplace transformation. In order to keep the inverse transformation tractable, we employ the fact that the boundary concentration $C_p(0,t)$ is practically constant when $t$ is not too large. In fact, without sorption, $C_p(0,t)$ begins to change appreciably from its initial value only after the flux at $z = a$ gains its maximum. Thus, in the case of finite $\lambda$ and $\mu$, we fix $C_p(0,t)$ to the nontrivial concentration obtained from Eq. (18) as $t \to 0^+$ (compare with Eq. 16).

$$C_p(0,0^+) = \frac{\phi C_0}{1 + \phi\sqrt{D/D_g}} \qquad (21)$$

Even after this approximation, the calculations are rather tedious and we do not reproduce them here. A very similar problem has been studied by Crank [7] and we refer to his book for the methods used.

## COMPARISON OF THE SIMULATIONS, ONE-DIMENSIONAL THEORY AND EXPERIMENTS

### Comparison of Simulations and Theory

When plotting the simulated and theoretical fluxes, we use the dimensionless time $t' = Dt/a^2$ and rescaled flux $H' = Ha/(C_0D)$. We determine the diffusion constant $D$ of the one-dimensional theory by matching the theoretical and simulated fluxes at long times. The comparison between theory and simulations then concerns the time evolution of the flux $H'(t')$. In free space, i.e. without the sheet, the flux obtained from simulations is indistinguishable from the solution of the one-dimensional theory.

We consider first the case of no sorption.

Figure 2a shows that the simulation and one-dimensional theory give the same time evolution of flux when the sheet is thick. Reducing the grammage increases the simulated diffusion constant (see the dashed curve in Fig. 2b). When we readjust the diffusion constant of the one-dimensional theory to match the long time flux (the solid curve in Fig. 2b), we find that the flux rises initially faster than the one-dimensional theory predicts. The discrepancy suggests that the one-dimensional diffusion theory cannot describe the time evolution of the diffusion flux through thin paper sheets.

The threshold grammage needed for the one-dimensional diffusion theory to be valid increases as porosity decreases, as demonstrated in Fig. 3. We have not analyzed the effect in detail, but at least the threshold grammage is much larger than the one [2,3] at which three-dimensional pores start to form in the network. The latter threshold levels are 20 g/m$^2$ for sheets of mechanical pulp and up to 50 g/m$^2$ for sheets of chemical pulp, and the corresponding porosities are 0.5 and down to 0.2, respectively.

Figure 4 shows how the simulated diffusion constant $D$ decreases when porosity decreases. At low porosities but high grammages, there will be a non-zero limiting porosity at which the flux becomes zero, as is apparent from the figure. In this limit, the flux is expected to vary from sample to sample much more than at intermediate or large porosities. Note that any kind of porosity gradients will have a complicating effect on such a threshold, whether one studies a real sheet or our computer-generated networks. In the simulations, the effective height-dependent porosity $\phi_{\mathrm{eff}}(z)$, defined as the porosity averaged in a window of small width around height $z$, takes some time to settle into the asymptotic bulk behaviour as the sheet thickness is increased. This follows naturally from the fact that one needs a few layers of fibres to have pores at all, and thus low grammage cases are more compact. If grammage is low, more or less direct holes

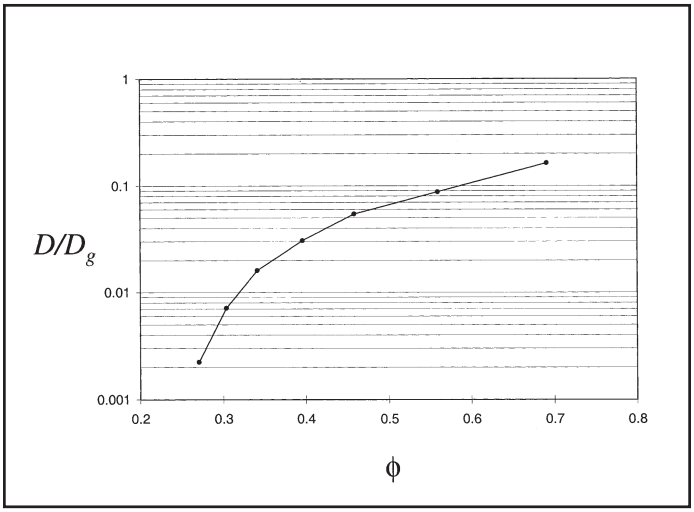


**Fig. 4. The diffusion constant $D$ as a function of porosity $\phi$ for a thick fibre network ($a$ > 130 μm).**

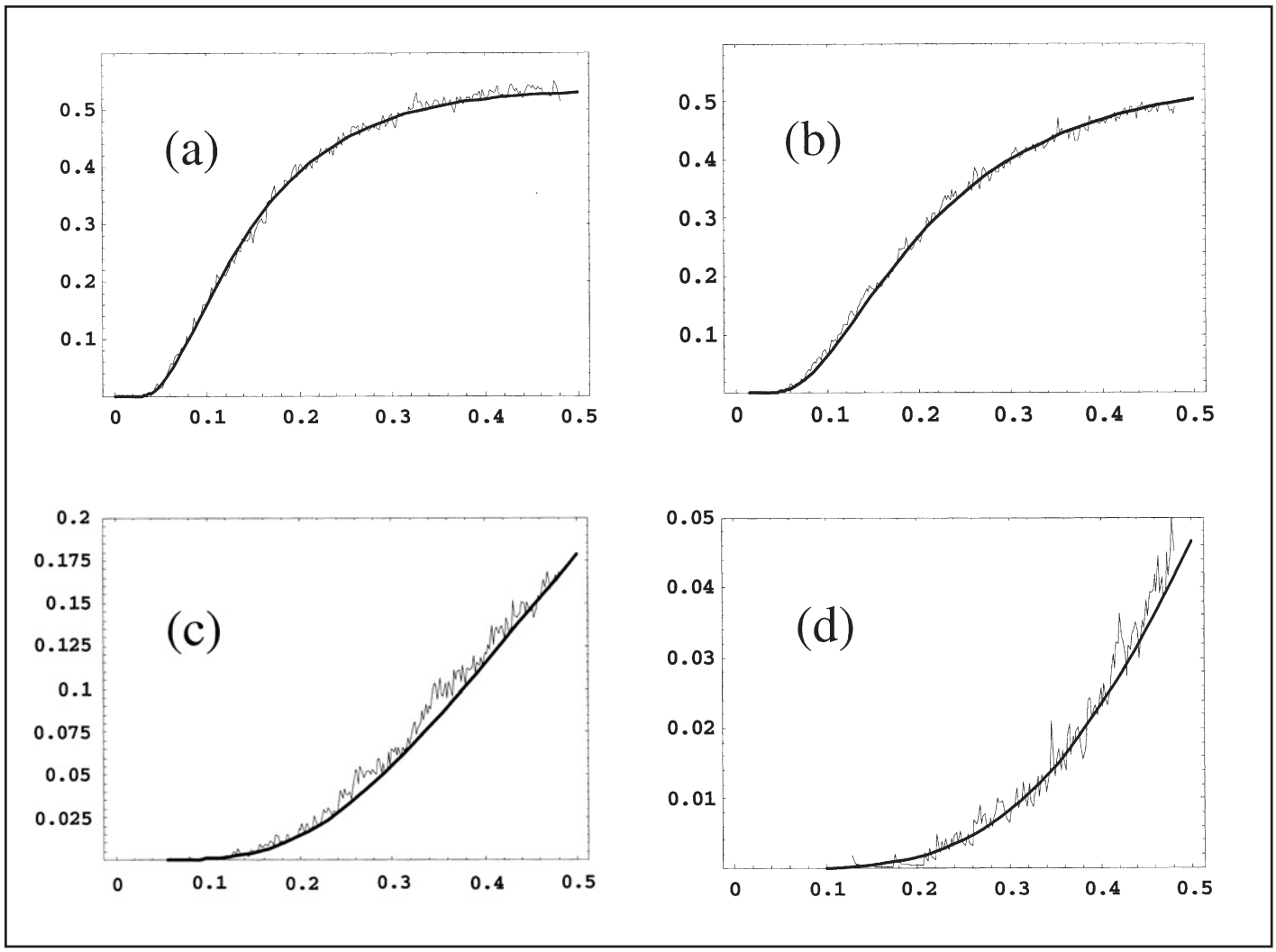


**Fig. 5. The effect of sorption on the flux rise for the sheet with $\phi_{app}$ = 0.691, $a$ = 582 μm, $D$ = 0.163 $D_g$. (a) $\hat{\nu}$ = 0 (no absorption), (b) $\hat{\nu}$ = 6, (c) $\hat{\nu}$ = 50, and (d) $\hat{\nu}$ = 100. In (b)–(d) $\lambda$ = 0.0002. The smooth line describes the one-dimensional theory and the rough one the simulations.**

through the sheet also cause variability from sample to sample.

When sorption is present, there are three free parameters $D$, $\lambda$, and $\mu$ in the one-dimensional theory. It is natural to assume that $D$ is the same as would be obtained for the same sheet without sorption. In other words, $D$ should be determined solely by the pore geometry and sheet thickness. The other two parameters, $\lambda$ and $\mu$, cannot be simply put equal to their counterparts, $\hat{\lambda}$ and $\hat{\mu}$ in the simulations, because the rate of sorption and desorption is different in the two models. In the simulations, sorption/desorption takes place only at fibre surfaces, but in the one-dimensional model it takes place in every volume element. As a result, $\lambda$ and $\mu$ will depend on the free fibre surface area and hence porosity in some unknown manner.

Figure 5 shows the comparison of the simulation and one-dimensional theory for a thick and relatively porous sheet ($\phi = 0.691$). After first adjusting the diffusion constant $D$ for $\hat{\nu} = 0$ as explained before, we determined the values $\lambda = 0.0002$ and $\mu = 2.68 \times 10^{-5}$ by matching the rising part of the simulated flux for $\hat{\nu} = 100$ with the one-dimensional theory. The good agreement is possible only when both $\lambda$ and $\mu$ are treated as adjustable parameters. In particular, the match is impossible if $\lambda = \mu = 0$, implying that the sorption and desorption terms in Eqs. (9) and (10) are essential.

We then repeated the same procedure for the other two cases, $\hat{\nu} = 6$ and $\hat{\nu} = 50$. A good match between the one-dimensional theory and the simulated flux (see Fig. 5) resulted when we kept the parameter $\lambda = 0.0002$ constant and calculated $\mu$ from

$$\frac{\lambda}{\mu} = \hat{\nu} S \tag{22}$$

Here, $S = 0.0746$ and $\hat{\nu} = \hat{\lambda} / \hat{\mu}$. The same values $\lambda = 0.0002$ and $S = 0.0746$ apply to other thicknesses, too, when porosity is constant. The physical interpretation of Eq. (22) is that $S$ characterizes the free specific surface area of fibres (i.e., free surface area divided by the pore volume). Indeed, when we lowered porosity, we had to increase the value of $S$ accordingly. For example, when $\phi \approx 0.46$, we obtain a good fit when $S = 0.1360$. The same value $\lambda = 0.0002$ could be used at all the porosities that we tested.

Grammage was reasonably high (above 100 g/m$^2$) in all the simulations considered here. It is probable that low grammages would require a different set of parameters in the one-dimensional theory to match simulations.

## Comparison with Experiments for Water Vapour

In experiments, one usually measures the effective diffusion constant $D_e$ describing the steady-state flux through the sheet. This flux can be written in terms of the concentrations above and below the sheet:

$$\text{Flux} = -D\frac{\partial C_p}{\partial z} = D_e \frac{C(z=0) - C(z=a)}{a} \tag{23}$$

where $D_e = \phi D$ is the effective diffusion constant. In the previous section, we determined the value of the diffusion constant $D$ by matching the simulated flux at long times with the one-dimensional diffusion theory. As the porosity $\phi$ is known in the simulations, we obtain readily an estimate of the effective diffusion constant $D_e$ as well.

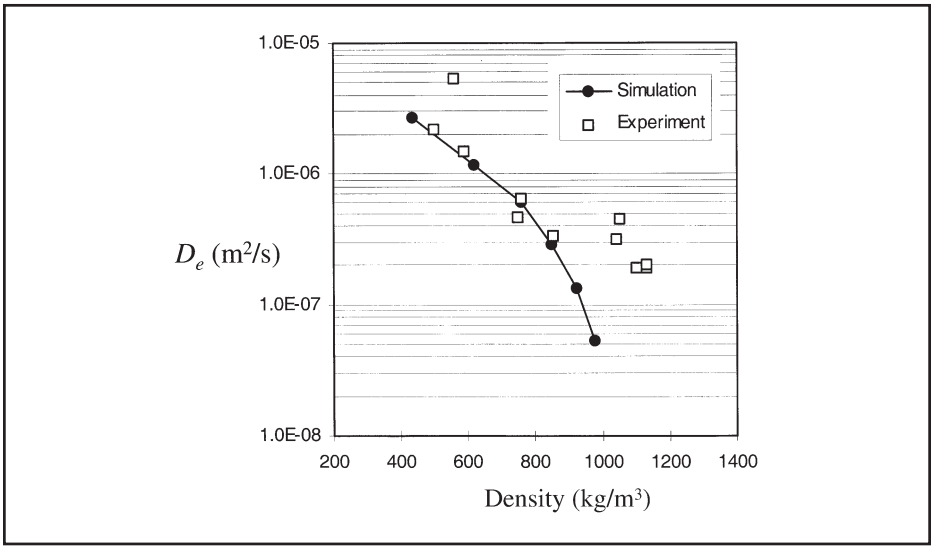


**Fig. 6. Comparison between the theoretical and experimental effective diffusion constants for water vapour as a function of the apparent sheet density. The experimental results have been obtained by Nilsson et al. [8] for various uncoated pulp and paper sheets. The theoretical values come from simulations with random fibre networks using the known value [10] $D_g = 0.242 \times 10^{-4}$ m$^2$/s for the diffusion of water molecules in air.**

Figure 6 shows the simulated effective diffusion constant together with values measured by Nilsson et al. [8] for water vapour in various uncoated pulp and paper samples. In a very recent work, Radhakrishnan et al. [9] obtained $D_e$-values which are close to those of Nilsson et al. The measurement times in the experiments by Nilsson et al. are so long that fibres can be assumed to be fully saturated. Thus, the simulations can be carried out without sorption. The simulated sheets have fairly large grammage (140–280 g/m$^2$). The fibre density value $\rho_f = 1400$ kg/m$^3$ and the diffusion constant [10] $D_g = 0.242 \times 10^{-4}$ m$^2$/s for $H_2O$–air mixture are used to rescale the dimensionless simulation results to physical units.

Because no attempts were made to reproduce the actual structure of the experimental sheets in the simulations, the comparison is only between orders of magnitudes. Still, the agreement is quite good, especially at low apparent densities which include hardwood and softwood pulp, liner and cardboard samples. Deviations between the experimental and simulation results take place for low-density filter paper and high-density writing paper, LWC base paper, newsprint, and sack paper. Some of these deviations can probably be explained by fillers increasing the apparent density.

## CONCLUSIONS

We have shown that the random walk simulations in KCL-PAKKA fibre networks can be used to obtain the effective parameters that describe the diffusion of gaseous compounds through paper and board sheets. The simulation results are consistent with steady-state experiments of water vapour diffusion through paper and board specimens.

When sorption effects can be ignored and sheet grammage is sufficiently high, the simulation results are also consistent with the one-dimensional diffusion theory. This means that the one-dimensional theory predicts correctly the entire time-evolution of diffusion flux through sheets of reasonable porosity and grammage. On the other hand, our results suggest that the one-dimensional diffusion theory is not valid at low porosities and low thicknesses. We have not determined the actual threshold levels in detail but rough estimates indicate, for example, that ordinary 60 g/m$^2$ handsheets are in practice always too thin for the one-dimensional diffusion theory to apply. In sheets made of chemical pulp (porosity ranging from 0.2 to 0.4), the minimum grammage probably exceeds 100 g/m$^2$. We emphasize that these are rough estimates.

We do not yet know the reasons why the one-dimensional diffusion theory fails at low porosities and low grammages. Statistical fluctuations in sheet structure are certainly one factor for low porosities. It is also possible that shallow pores between almost parallel flat fibre surfaces act as traps inside which the molecules have to bounce for a long time before escaping. Their effect on the time-dependent diffusion flux would be qualitatively the same as that of sorption. At low grammages fast, almost straight channels through the sheet can cause the initial flux to rise faster than the one-dimensional theory predicts.

Sorption and desorption are other factors that complicate the use of the one-dimensional diffusion theory. Sorption slows down the initial diffusion through the sheet but does not alter the steady-state flux. The retarded flux rise cannot be described simply by lowering the diffusion constant in the one-dimensional diffusion theory because the steady-state flux at long times is independent of sorption and

desorption. When sorption and desorption are included in the one-dimensional theory, two parameters $\lambda$ and $\mu$ enter that depend not only on the sorption-desorption properties of the fibres but also on the porous structure of the sheet. This means that, if sorption is relevant, steady-state measurements of the diffusion constant combined with the one-dimensional diffusion theory are not enough to predict the dynamic evolution of diffusion flux.

The deviations from one-dimensional diffusion flux are very important because the cases of practical interest are often dynamic. Computer simulations are one way to analyze such processes. The requirement of high grammage is particularly relevant for uncoated greaseproof paper and glassine that are used in food packaging [11]. Due to the low porosity, these materials have very small effective diffusion constants and they act as good barriers. On the other hand, their thickness is typically not very large, so that the one-dimensional diffusion theory is probably invalid.

We have concentrated here on diffusion in sheets consisting only of one fibre type. It would be straightforward to include many fibre types with varying geometric dimensions and sorption characteristics and, for example, study how to optimize the penetration characteristics as the mixture properties are varied.

## APPENDIX A: FIRST PASSAGE DISTRIBUTION IN FREE SPACE

Consider a random walk in a three-dimensional cubic lattice with the lattice constant set to unity. The aim is to calculate the first-passage time distribution into the plane $z = 0$ when the walker starts from the site $(x, y, z) = (0, 0, -z_0)$, $z_0 > 0$, at time $n = 0$. Here $n$ denotes the number of steps. Let $P_{z_0}(n)$ denote the probability that the first passage through the plane $z = 0$ occurs at the step number $n$. Due to the special symmetry of the problem, the calculation reduces to the properties of a one-dimensional random walk in the $z$-direction since

$$P_{z_0}(n) = \sum_{n_z} P(n_z|n) P^{1d}_{z_0}(n_z) \tag{24}$$

where $P(n_z|n)$ is the probability that $n_z$ out of $n$ steps are in the z-direction and

$$P^{1d}_{z_0}(n_z)$$

is the one-dimensional first passage probability to the distance $z_0$ from the starting point. The probability to jump into the z-direction is $p_z = 1/3$ and to perpendicular directions $p_{xy} = 2/3$. The distribution $P(n_z|n)$ is binomial

$$P(n_z|n) = \binom{n}{n_z} p_z^{n_z} p_{xy}^{n-n_z} \tag{25}$$

The first-passage probability for a one-dimensional random walk which starts from $z$ and goes through $z = 0$ at the step $2n_z - z_0$ is [12]

$$\frac{z_0}{2n_z - z_0}\binom{2n_z - z_0}{n_z} 2^{-(2n_z - z_0)} \tag{26}$$

Combining Eqs. (24)–(26) leads to Eq. (6)

$$\begin{aligned} P_{z_0}(n) &= \sum_{n_z = z_0}^{\lceil (n+z_0)/2 \rceil} \frac{z_0}{2n_z - z_0}\binom{2n_z - z_0}{n_z} \\ &\times 2^{-(2n_z - z_0)}\binom{n-1}{2n_z - z_0 - 1} \\ &\times p_z^{2n_z - z_0} p_{xy}^{n-(2n_z - z_0)} \\ &= \left(\frac{2}{3}\right)^n z_0 4^{z_0} \sum_{n_z = z_0}^{\lceil (n+z_0)/2 \rceil} \\ &\times \frac{4^{-2n_z}(n-1)!}{n_z!(n_z - z_0)!(n - 2n_z + z_0)!} \end{aligned} \tag{27}$$

where $\lceil x \rceil$ denotes the integer part of $x$ and $n - 1$ instead of $n$ in the combinatorial factor takes into account the fact that the last step has to be from $z = -1$ to $z = 0$. The function $Pz_0(n)$ is peaked around $z_0^2$ and decays as $n^{-3/2}$ for $n >> z_0^2$.

Equation (27) is not handy for large values of $n$. Therefore, in the simulations we use the continuum approximation $p_{z_0}(t)$ for $P_{z_0}(n)$ when n > 1500 (Eq. 7). This can be obtained by solving the diffusion equation

$$\frac{\partial U}{\partial t} = d\nabla^2 U \tag{28}$$

where $d$ is the diffusion constant and $U(x, y, z; t)$ is the probability density function for the position of the walker relative to the origin at time $t$, without ever crossing the boundary $z = 0$. The boundary and initial conditions are $U(x, y, z = 0; t) = 0$ and $U(x, y, z; 0) = \delta(x - x_0)\,\delta(y - y_0)\,\delta(z - z_0)$, respectively. Without loss of generality, we can set $x_0 = y_0 = 0$. The solution can be obtained using the familiar image method [12]. For $z \geq 0$, the solution is the superposition of a Gaussian centred at $(0, 0, z_0)$ and an image anti-Gaussian at $(0, 0, -z_0)$:

$$\begin{aligned} U(x, y, z; t) &= (4\pi d\mathrm{t})^{-3/2} \\ &\times \left[\mathrm{e}^{-(x^2 + y^2 + (z - z_0)^2)/4dt}\right. \\ &\left. - \mathrm{e}^{-(x^2 + y^2 + (z + z_0)^2)/4dt}\right] \end{aligned} \tag{29}$$

The first passage probability through the point $(x, y, 0)$ is obtained from the flux

$$\begin{aligned} p_{z_0}(x, y; t) &= d\left.\frac{\partial U}{\partial z}\right|_{z=0} \\ &= z_0(4\pi d)^{-3/2} t^{-5/2} \mathrm{e}^{-(x^2 + y^2 + z_0^2)/4dt} \end{aligned} \tag{30}$$

from which the flux through the plane $z = 0$ is obtained by integrating over $x$ and $y$:

$$p_{z_0}(t) = \frac{z_0}{\sqrt{4\pi d}} t^{-3/2} \mathrm{e}^{-z_0^2/4dt} \tag{31}$$

This is exactly the same distribution as in one dimension except that the diffusion constant in three dimensions is $d = 1/6$.

## APPENDIX B: SPATIAL DISTRIBUTION

Let a random walker start from $z = -1$ at the time $n = 0$ and reach the plane $z = 0$ for the first time at the step $n$. To calculate the spatial distribution in the plane $z = 0$ it is convenient to consider the steps in the z direction and in the xy plane separately. First consider a two-dimensional random walk. Let $n_x^-$, $n_x^+$, $n_y^-$, and $n_y^+$ denote the number of steps in the negative and positive x and y directions, respectively, and let the total number of steps be $n$. The probability $\mathrm{P}(n_x^-, n_x^+, n_y^-, n_y^+)$ is multinomially distributed and the number of walks for given $n_x^-$, $n_x^+$, $n_y^-$, and $n_y^+$ is

$$\pi_n(n_x^-, n_x^+, n_y^-, n_y^+) = \frac{n!}{n_x^-!\,n_x^+!\,n_y^-!\,n_y^+!} \tag{32}$$

Now we are interested only in the position $x(n) = r$, $y(n) = s$ after the $n$th step assuming $x(0) = y(0) = 0$. We have the constraints

$$\begin{cases} n = n_x^- + n_x^+ + n_y^- + n_y^+ \\ r = n_x^+ - n_x^- \\ s = n_y^+ - n_y^- \end{cases} \tag{33}$$

which can be used to write the number of walks as $\pi_n(n_x^+, r, s)$. The total number of walks ending at the point $(r, s)$ is obtained by summing this over $n_x^+$ (see Eq. 34) where $r$ and $s$ must obey the constraints

$$\begin{cases} 0 \leq r \leq n \\ 0 \leq s \leq r \\ r + s \leq n \\ n + r - s \text{ even} \end{cases} \tag{35}$$

In fact, Eq. (34) gives the result everywhere since the walk is symmetric so that $\prod_n(\pm r, \pm s) = \prod_n(r, s)$ and for $n + r - s$ odd, $\prod_n(r, s) = 0$.

For a three-dimensional random walk, the spatial distribution in the plane $z = 0$ can be obtained by taking into account all the combinations which have their endpoints in this plane. We can thus utilize the one-dimensional result given by Eq. (26) together with the above result for spatial distribution in the xy plane, Eq. (34), to get the number of walks for which the walker is at $(r, s, 0)$ at the step $n$ so that $z(m) < 0 \ \forall m < n$:

$$\begin{aligned} \Phi_n(r, s) &= \sum_{j=0}^{\lceil (n-1)/2 \rceil} \binom{n-1}{2j} \frac{1}{2j+1} \\ &\times \binom{2j+1}{j} \prod_{n-1-2j}(r, s) \end{aligned} \tag{36}$$

The first combinatorial factor counts the number of possible ways to have $2j$ z-directional

**Equation 34**

$$\prod_n(r, s) = \sum_{n_x^+ = r}^{(n+r-s)/2} \frac{n!}{(n_x^+ - r)!\,n_x^+!\,[(n+r-s)/2 - n_x^+]!\,[(n+r+s)/2 - n_x^+]!}$$

steps among $n-1$ steps (again the last step has to be from $z=-1$ to $z=0$). The corresponding probability is

$$P_n(r,s)=\frac{\Phi_n(r,s)}{\sum_{r,s}\Phi_n(r,s)}=\frac{\Phi_n(r,s)}{6^n P_1(n)} \tag{37}$$

where the last form has been obtained using Eq. (27).

Similarly as for $P_{z_0}(n)$, we approximate $P_n(r, s)$ by its continuous counterpart for large $n$. In the simulations, we first calculate the time $t$ at which we come to the plane $z=0$ when leaving from $z_0=1$. Equation (30) gives

$$p_1(x,y;t)=(2\pi/3)^{-3/2}t^{-5/2}\mathrm{e}^{-3(x^2+y^2+1)/2t} \tag{38}$$

Changing to the polar coordinates $[p_1(x,y;t)\mathrm{d}x\mathrm{d}y = p_1(R,\phi;t)R\mathrm{d}R\mathrm{d}\phi]$ and integrating over $\phi$, we get Eq. (8).

## ACKNOWLEDGEMENTS

We thank B. Aurela, S. Chatterjee, B. Ramarao, and S. Stenström for useful discussions. This work has been partly funded by the National Technology Agency (TEKES).

## REFERENCES

1. CRANK, J., The Mathematics of Diffusion, 2nd ed., Oxford University Press, Oxford (1975).
2. NISKANEN, K.J. and ALAVA, M.J., "Planar Random Networks with Flexible Fibers", *Phys. Rev. Lett.* 73(25):3475–3478 (1994).
3. HELLÉN, E.K.O, ALAVA, M.J. and NISKANEN, K.J., "Porous Structure of Thick Fiber Webs", *J. Appl. Phys.* 81(9):6425–6431 (1997).
4. MacKEOWN, P. K., Stochastic Simulation in Physics, 1st ed., Springer, Singapore, Ch. 8 (1997).
5. TAYLOR, H.M. and KARLIN, S., "An Introduction to Stochastic Modeling", 1st ed., Academic Press, Inc., Orlando, Sec. 3.4 (1984).
6. CARSLAW, H.S. and JAEGER, J.C., Conduction of Heat in Solids, 2nd ed., Oxford University Press, Oxford, Sec. 12.8 (1959).
6. CRANK, J., The Method of Diffusion, 2nd ed., Oxford University Press, Section 14.4 (1975).
7. NILSSON, L., WILHELMSSON, B. and STENSTRÖM, S., The Diffusion of Water Vapour through Pulp and Paper, *Drying Techn.* 11(6):1205–1225 (1993).
8. RADHAKRISHNAN, H., CHATTERJEE, S.G. and RAMARAO, B.V., "Steady-State Moisture Transport in a Bleached-Kraft Paperboard Stack", *J. Pulp Paper Sci.* 26(4):140–144 (2000).
9. CRC Handbook of Chemistry and Physics, 75th ed., CRC Press, Boca Raton (1994).
10. SÖDERHJELM, L. and SIPILÄINEN-MALM, T., "Paper and Board" in Migration from Food Contact Materials, L. L. Katan, Ed., Chapman & Hall, 159–180, (1996).
11. FELLER, W., An Introduction to Probability Theory and its Applications, 1st ed., John Wiley & Sons, New York, II:59 (1966).
12. WEISS, G.H., Aspects and Applications of the Random Walk, 1st ed., North-Holland, Amsterdam, 171 (1994).

**REFERENCE:** HELLÉN, E.K.O., KETOJA, J.A., NISKANEN, K.J. and ALAVA, M.J., Diffusion through Fibre Networks. Journal of Pulp and Paper Science, 28(2):55–62 February 2002. Paper offered as a contribution to the Journal of Pulp and Paper Science. Not to be reproduced without permission from the Pulp and Paper Technical Association of Canada. Manuscript received May 16, 2000; revised manuscript approved for publication by the Review Panel June 12, 2001.

**KEYWORDS:** AS, DIFFUSION, FIBER NETWORKS, SIMULATION, STEADY STATE, POROSITY, THICKNESS, SORPTION.